

Chapter 2

Multi-DoF Interface Synchronization of Real-Time-Hybrid-Tests Using a Recursive-Least-Squares Adaption Law: A Numerical Evaluation

Andreas Bartl, Johannes Mayet, Morteza Karamooz Mahdiabadi, and Daniel J. Rixen

Abstract Cyber Physical Testing or Real Time Hybrid Testing is a Hardware-In-The-Loop approach allowing for tests of structural components of complex machines with realistic boundary conditions by coupling virtual components. The need to actuate the physical interface makes the tests on structural systems challenging. In order to deal with stability and accuracy issues, we propose the use of an Adaptive Feed-Forward Cancellation approach with a Recursive Least Squares (RLS) adaption law for interface synchronization of harmonically excited systems. The interface forces are generated from multiple harmonic components of the excitation force. A RLS adaption law sets the amplitudes and phases of the harmonic interface force components and minimizes the interface gap. One major practical advantage of using a RLS adaption law is that only one forgetting factor has to be chosen compared to other adaption algorithms with various tuning parameters. As a consequence, it is possible to test systems with multiple interface DoF. In order to illustrate the performance and robustness of the proposed testing algorithm, the contribution includes a numerical investigation on a lumped mass system.

Keywords Hybrid testing • Hardware-in-the-loop • Real-time substructuring • Interface synchronization • Recursive least squares

2.1 Introduction

Real Time Hybrid Testing, Cyber Physical Testing or Hardware-in-the-Loop for structural systems is a testing approach connecting experimental test rigs (experimental component) with simulation models (virtual component) in a real time test (see Figs. 2.1 and 2.2). In contrast of testing the experimental component by applying fictitious load cases, realistic boundary conditions are provided in these test procedures. The approach is always valuable where neither full experimental tests nor full simulations are applicable. Real Time Hybrid Testing was applied in engineering of earthquake safe civil structures in [3, 12, 17]. A testing example on a full wind turbine nacelle is presented in [6] and an automotive application is given in [18].

The objective of the interface synchronization control in Real Time Hybrid Testing (RTHT) is to satisfy equilibrium and compatibility constraints within the desired frequency range. Consider for example structural applications with commonly low damping of the overall system. Controlling a system with poles close to the imaginary axis can cause instability of the real time test due to small control errors and inaccuracies in measurement or actuation. The problem of interface synchronization is closely linked to actual compensation methods. The performance of actuator compensation methods is compared in [5]. The authors of [15, 21] present frameworks for the development of RTHT controllers. A Linear-Quadratic-Regulator controller framework is presented in [22]. In the contribution [7] the Real Time Hybrid Testing problem is analyzed with conventional control theory. As in many applications the dynamics of the experimental substructures are unknown, Model Reference Adaptive Control (MRAC) is proposed as a control strategy in [19, 23]. A widely used approach is based on polynomial forward prediction used in [8, 12] for compensation of the actuator dynamics. The authors of [24] extend this approach by gain and phase estimation. More recently neuronal network feedforward compensation for the use in Real Time Hybrid Testing were proposed in [16]. Model Predictive Control is proposed as a control strategy for RTHT in [20].

In [1] we presented a adaptive feedforward algorithm with a harmonic regressor (see e.g. [2, 4, 10]) applied to RTHT. The adaption is based on a gradient algorithm. This approach is closely linked to fXLMS Algorithm as presented in [14]. However, in case of multiple DoF interfaces the choice of the adaption gain matrix, which defines the stability of the algorithm, is getting impractical. The entries of the adaption gain matrix can vary within several orders of magnitude and wrong choices may cause instability of the test. Therefore, we propose in this contribution an adaptive feedforward filter with harmonic

A. Bartl (✉) • J. Mayet • M.K. Mahdiabadi • D.J. Rixen
Technical University of Munich, Boltzmannstraße 15, D-85748 Garching, Germany
e-mail: andreas.bartl@tum.de

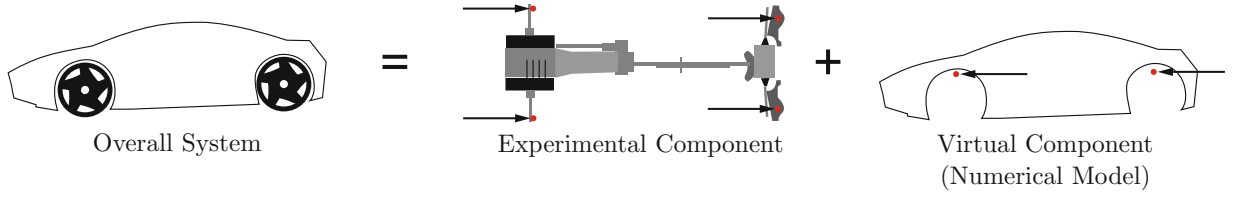


Fig. 2.1 The overall system is split into a virtual and an experimental component

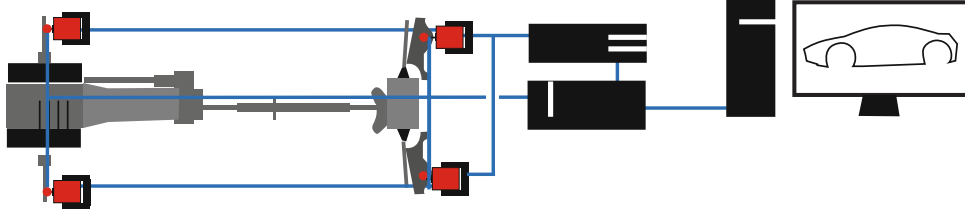


Fig. 2.2 The test rig is coupled with sensors and actuators to the virtual component running on a real time computer

regressor based on a Recursive Least Squares (RLS) adaption law with only a single tuning parameter. The fact that the user has only to choose one tuning parameter makes the suggested approach applicable to carry out various tests on systems with a multi DoF interface.

2.2 Hybrid Testing Problem Formulation

The objective of the RTHT control is to satisfy compatibility (Eq. (2.1)) and equilibrium (Eq. (2.2)) constraints between virtual and experimental components. The Boolean matrices G_V and G_E are selecting the interface forces and displacements (see [9] for details). $y_{b,V}$ and $y_{b,E}$ are the interface displacement vectors. The interface gap is denoted as e . $f_{b,V}$ and $f_{b,E}$ are the interface force vectors

$$G_V u - G_E u = y_{b,V} - y_{b,E} = e = 0 \quad (2.1)$$

$$G_V f_{b,V} + G_E f_{b,E} = 0 \quad (2.2)$$

In principal two distinctive ways for setting up an control scheme do exist. One possibility is to define the interface displacements as compatible and controlling the interface forces in order to achieve equilibrium. In contrast one can define the interface forces as forces with equal magnitude and opposite sign, controlling the interface gap. In this contribution, we use the latter one, which is comparable to the to the dual formulation in substructuring (see [9] for details). In practice, this foregoing is absolutely meaningful since one will end up with forces as controller setpoint rather than gaps which would necessarily require inner-loop actuator control algorithms. The applied forces λ are subsequently measured and applied to the virtual subcomponent with opposite sign. The dynamics of both components are given by Eq. (2.3).

$$\begin{bmatrix} M_V & 0 \\ 0 & M_E \end{bmatrix} \begin{bmatrix} \ddot{u}_V \\ \ddot{u}_E \end{bmatrix} + \begin{bmatrix} D_V & 0 \\ 0 & D_E \end{bmatrix} \begin{bmatrix} \dot{u}_V \\ \dot{u}_E \end{bmatrix} + \begin{bmatrix} K_V & 0 \\ 0 & K_E \end{bmatrix} \begin{bmatrix} u_V \\ u_E \end{bmatrix} + \begin{bmatrix} G_V^T \\ -G_E^T \end{bmatrix} \lambda = \begin{bmatrix} f_V \\ f_E \end{bmatrix} \quad (2.3)$$

The objective of an interface synchronization controller will be to apply λ such that the interface gap e is closed. The assumptions of the control strategy are an harmonic excitation and steady-state system behaviour. The block diagram of the overall control system is given in Fig. 2.3. Before deriving the algorithm the hybrid testing problem is reformulated such that it can be used for an adaptive feedforward compensator in this section. The corresponding state space formulations are given in Eqs. (2.4) and (2.5).

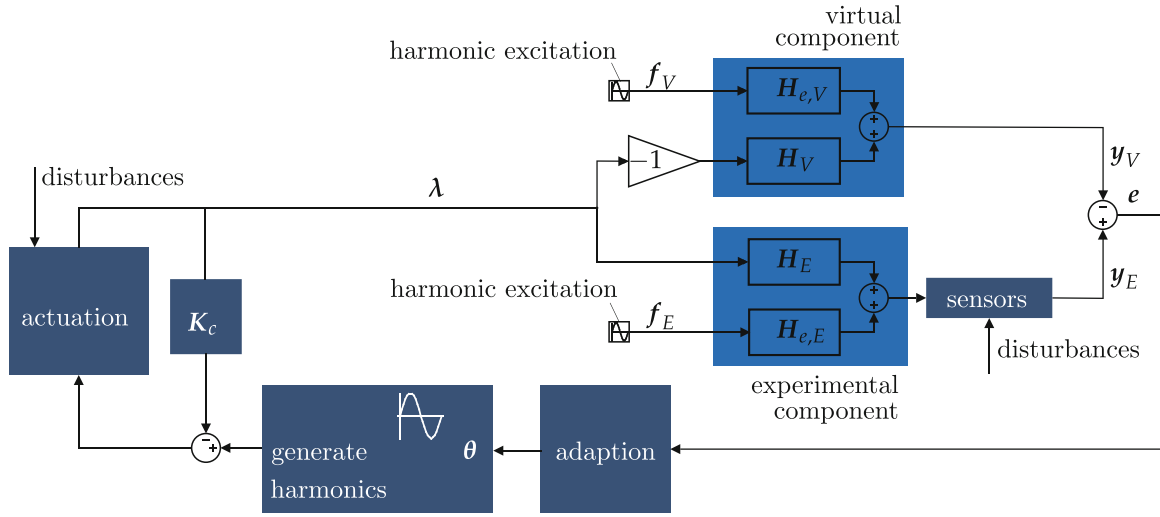


Fig. 2.3 The block diagram shows the hybrid test with adaptive feedforward compensation. Harmonic excitation on both the experimental and virtual component are possible. The actuator is exciting the experimental and contrariwise the virtual component in the present of real and virtual harmonic excitations. The controller adapts phase and gain of the harmonic inputs to the actuator such that the interface gap e is closed. (adapted from [1])

$$\dot{x}_V = \underbrace{\begin{bmatrix} \mathbf{0} & \mathbf{I} \\ -\mathbf{M}_V^{-1}\mathbf{K}_V & -\mathbf{M}_V^{-1}\mathbf{D}_V \end{bmatrix}}_{\mathbf{A}_V} x_V + \underbrace{\begin{bmatrix} \mathbf{0} \\ \mathbf{M}_V^{-1}\mathbf{G}_V^T \end{bmatrix}}_{\mathbf{B}_V} \lambda + \underbrace{\begin{bmatrix} \mathbf{0} \\ \mathbf{M}_V^{-1} \end{bmatrix}}_{\mathbf{E}_V} f_V \quad (2.4)$$

$$y_V = \mathbf{G}_V \mathbf{u}_V = \underbrace{\begin{bmatrix} \mathbf{G}_V & \mathbf{0} \end{bmatrix}}_{\mathbf{C}_V} x_V$$

$$\dot{x}_E = \underbrace{\begin{bmatrix} \mathbf{0} & \mathbf{I} \\ -\mathbf{M}_E^{-1}\mathbf{K}_E & -\mathbf{M}_E^{-1}\mathbf{D}_E \end{bmatrix}}_{\mathbf{A}_E} x_E - \underbrace{\begin{bmatrix} \mathbf{0} \\ \mathbf{M}_E^{-1}\mathbf{G}_E^T \end{bmatrix}}_{\mathbf{B}_E} \lambda + \underbrace{\begin{bmatrix} \mathbf{0} \\ \mathbf{M}_E^{-1} \end{bmatrix}}_{\mathbf{E}_E} f_E \quad (2.5)$$

$$y_E = \mathbf{G}_E \mathbf{u}_E = \underbrace{\begin{bmatrix} \mathbf{G}_E & \mathbf{0} \end{bmatrix}}_{\mathbf{C}_E} x_E$$

The interface responses can be written as

$$y_V = \underbrace{\int_{t_0}^t \mathbf{C}_V e^{\mathbf{A}_V(t-\tau)} \mathbf{B}_V \lambda d\tau}_{\text{contribution of interface excitation with transfer function } \mathbf{H}_V(j\omega)} + \underbrace{\int_{t_0}^t \mathbf{C}_V e^{\mathbf{A}_V(t-\tau)} \mathbf{E}_V f_V d\tau}_{\text{contribution of external excitation}} + \underbrace{\mathbf{C}_V e^{\mathbf{A}_V(t-\tau)} \mathbf{x}_V(t_0)}_{\text{contribution of initial conditions}} \quad (2.6)$$

$$y_E = \underbrace{\int_{t_0}^t \mathbf{C}_E e^{\mathbf{A}_E(t-\tau)} \mathbf{B}_E \lambda d\tau}_{\text{contribution of interface excitation with transfer function } \mathbf{H}_E(j\omega)} + \underbrace{\int_{t_0}^t \mathbf{C}_E e^{\mathbf{A}_E(t-\tau)} \mathbf{E}_E f_E d\tau}_{\text{contribution of excitation}} + \underbrace{\mathbf{C}_E e^{\mathbf{A}_E(t-\tau)} \mathbf{x}_E(t_0)}_{\text{contribution of initial conditions}} \quad (2.7)$$

Assuming harmonic excitations and steady state behavior, the contribution of initial conditions are neglected. The interface forces can be expressed as a combination of harmonic functions:

$$\lambda = \sum_{i=1}^m \mathbf{W}_i(t) \theta_i \quad (2.8)$$

$$\mathbf{W}_i(t) = [\mathbf{I}_{nn} \cos(\alpha_i) \quad \mathbf{I}_{nn} \sin(\alpha_i)] \quad \text{with} \quad \mathbf{W}_i \in \mathbb{R}^{n \times 2n}$$

In Eq. (2.8) the regressor matrix $W_i(t)$ contains the amplitudes for the cosine and sine part of the interface forces and thus the phase angle $\alpha_i = \int_0^t \omega_i(t)dt$ and frequency $\omega_i(t)$, which are allowed to vary slowly. The important parameter vector θ_i defines the phases and amplitudes of the interface forces. Since we assume steady state behavior y_V and y_E can now be rewritten as

$$y_V = \sum_{i=1}^m \underbrace{W_i(t)P_{V,i}\theta_i}_{\text{influence interface forces}} + \underbrace{W_i(t)\pi_{V,i}}_{\text{influence external excitation (disturbance)}} = W(t)P_V\theta + \sum_{i=1}^m W_i(t)\pi_{V,i} \quad (2.9)$$

$$y_E = \sum_{i=1}^m \underbrace{W_i(t)P_{E,i}\theta_i}_{\text{influence interface forces}} + \underbrace{W_i(t)\pi_{E,i}}_{\text{influence external excitation (disturbance)}} = W(t)P_E\theta + \sum_{i=1}^m W_i(t)\pi_{E,i}, \quad (2.10)$$

where the matrices $P_{V,i}$ and $P_{E,i}$ are created using transfer function $H_V(j\omega_1)$ and $H_E(j\omega_1)$ respectively (see Fig. 2.3 and Eqs. (2.11) and (2.12)). These matrices basically apply a phase shift and gain to the parameter vector θ . The vectors $\pi_{V,i}$ and $\pi_{E,i}$ define phase and amplitude of the contributions of the external forces to the interface displacements.

$$P_{V,i} = \begin{bmatrix} \text{Re}(H_V(j\omega_i)) & \text{Im}(H_V(j\omega_i)) \\ -\text{Im}(H_V(j\omega_i)) & \text{Re}(H_V(j\omega_i)) \end{bmatrix} = \begin{bmatrix} P_{R,V,i} & P_{I,V,i} \\ -P_{I,V,i} & P_{R,V,i} \end{bmatrix} \quad \text{with } P_{V,i} \in \mathbb{R}^{2n \times 2n} \quad (2.11)$$

$$P_{E,i} = \begin{bmatrix} \text{Re}(H_E(j\omega_i)) & \text{Im}(H_E(j\omega_i)) \\ -\text{Im}(H_E(j\omega_i)) & \text{Re}(H_E(j\omega_i)) \end{bmatrix} = \begin{bmatrix} P_{R,E,i} & P_{I,E,i} \\ -P_{I,E,i} & P_{R,E,i} \end{bmatrix} \quad \text{with } P_{E,i} \in \mathbb{R}^{2n \times 2n} \quad (2.12)$$

2.3 Adaptive Feedforward Algorithm

In order to couple virtual and experimental components, the parameter vector θ has to be chosen such that the interface gap e is closed. In order to adapt θ online, the use of a recursive least squares algorithm (see e.g. [11, 13]) is proposed, which minimizes the integral cost functional J defined in Eq. (2.13). Note that for the derivation of the adaption law, the above mentioned functions are used in their time discretized form. Here we use brackets to indicate a specific time instance. The cost functional includes a forgetting factor $\mu \in [0, 1]$, which enables a decreasing weighting of old values of $e^T[i]e[i]$ at i th time instances. The phase and gain matrices P_E and P_V as well as P_A , which characterizes the actuator dynamics, are combined to P .

$$J[k] = \sum_{i=0}^k \mu^{k-i} e^T[i]e[i] \quad (2.13)$$

with $e[i] = y_E[i] - y_V[i] = W[i] \underbrace{(P_E - P_V)P_A}_{P} \theta[i] + W[i] \underbrace{(\pi_E[i] - \pi_V[i])}_{\pi[i]}$

Starting point for deriving the adaption law for the hybrid testing problem is the solution of the least squares problem, which is then rearranged as recursive algorithm:

$$0 = \frac{\partial J[k]}{\partial \theta[k]} = \sum_{i=0}^k 2\mu^{k-i} (P^T W[i]^T W[i] P \theta[k] + P^T W[i]^T W[i] \pi[i]) \quad (2.14)$$

$$\theta[k] = \underbrace{\left(\sum_{i=0}^k \mu^{k-i} P^T W[i]^T W[i] P \right)^{-1}}_{R[k]} \left(\sum_{i=0}^k -\mu^{k-i} P^T W[i]^T W[i] \pi[i] \right) \quad (2.15)$$

The solution of the least squares problem for the next time step $k + 1$ is arranged as follows:

$$\theta[k + 1] = \left(\overbrace{\sum_{i=0}^k \mu^{k+1-i} \mathbf{P}^T \mathbf{W}[i]^T \mathbf{W}[i] \mathbf{P} + \mathbf{P}^T \mathbf{W}[k + 1]^T \mathbf{W}[k + 1] \mathbf{P}}^{\mathbf{R}[k+1]} \right)^{-1} \cdot \left(\sum_{i=0}^k -\mu^{k+1-i} \mathbf{P}^T \mathbf{W}[i]^T \mathbf{W}[i] \boldsymbol{\pi}[i] - \mathbf{P}^T \mathbf{W}[k + 1]^T \mathbf{W}[k + 1] \boldsymbol{\pi}[k + 1] \right)$$

Applying the Woodbury matrix identity allows to replace the inverse of the regressor matrix:

$$\theta[k + 1] = \left(\overbrace{\frac{1}{\mu} \mathbf{R}[k] - \frac{1}{\mu} \mathbf{R}[k] \mathbf{P}^T \mathbf{W}[k + 1]^T \left(\mathbf{I} + \frac{1}{\mu} \mathbf{W}[k + 1] \mathbf{P} \mathbf{R}[k] \mathbf{P}^T \mathbf{W}[k + 1]^T \right)^{-1} \mathbf{W}[k + 1] \mathbf{P} \mathbf{R}[k]}^{\mathbf{R}[k+1]} \right)^{-1} \cdot \left(\sum_{i=0}^k -\mu \mu^{k-i} \mathbf{P}^T \mathbf{W}[i]^T \mathbf{W}[i] \boldsymbol{\pi}[i] - \mathbf{P}^T \mathbf{W}[k + 1]^T \mathbf{W}[k + 1] \boldsymbol{\pi}[k + 1] \right)$$

Further simplification of the equations finally yields the recursive least squares adaption law:

$$\boldsymbol{\gamma}[k + 1] = \frac{1}{\mu} (\mathbf{R}[k] \mathbf{P}^T \mathbf{W}[k + 1]^T) (\mathbf{I} + \frac{1}{\mu} \mathbf{W}[k + 1] \mathbf{P} \mathbf{R}[k] \mathbf{P}^T \mathbf{W}[k + 1]^T)^{-1} \quad (2.16)$$

$$\theta[k + 1] = \theta[k] + \boldsymbol{\gamma}[k + 1] \underbrace{(\mathbf{W}[k + 1] \mathbf{P} \theta[k] + \mathbf{W}[k + 1] \boldsymbol{\pi}[k + 1])}_{\mathbf{e}'[k+1]} \quad (2.17)$$

$$\mathbf{R}[k + 1] = \frac{1}{\mu} (\mathbf{R}[k] - \boldsymbol{\gamma}[k + 1] \mathbf{W}[k + 1] \mathbf{P} \mathbf{R}[k]) \quad (2.18)$$

Note that \mathbf{e}' is the a-priori gap, which can be measured, whereas \mathbf{e} is the a-posteriori interface gap, which is used in the cost functional J . The RLS algorithm allows the practical application of adaptive feedforward compensation in Real Time Hybrid Testing with multiple DoF interfaces as a single forgetting factor μ has to be chosen. Note that the phase and gain matrix \mathbf{P} characterizing plant dynamics are used in the adaption law. \mathbf{P} can be identified prior to the adaption process by exciting each actuation DoF separately or with uncorrelated noise.

2.4 Numerical Case Study

The algorithm is applied to a simple lumped mass problem with a two DoF interface. The arrangement of the masses is illustrated in Fig. 2.4. The mass and stiffness parameters are given in Table 2.1. Proportional damping with a stiffness proportional coefficient $\alpha = 0.01$ and a mass proportional coefficient $\beta = 0.001$ is used, which confers a modal damping of 0.5 % to the submodels. The models and the interface synchronization control were implemented in Matlab[®] Simulink[®]. The excitation force $f_{V,ext} = \sum_{i=1}^4 A_i \sin \omega_i t$ was applied on mass 1. The excitation frequencies were $\omega_1 = 20 \frac{1}{\text{rad}}$, $\omega_2 = 30 \frac{1}{\text{rad}}$, $\omega_3 = 50 \frac{1}{\text{rad}}$ and $\omega_4 = 60 \frac{1}{\text{rad}}$. The amplitudes $A_1 = 4 \text{ N}$, $A_2 = 10 \text{ N}$, $A_3 = 10 \text{ N}$ and $A_4 = 20 \text{ N}$. The forgetting factor for the RLS algorithm was chosen as $\mu = 0.99$. The identification was running for 10 s with an excitation of 5 s on each actuation DoF. The adaption with the RLS algorithm starts at $t = 10 \text{ s}$.

Figures 2.5 and 2.6 show the interface synchronization for both interface DoF. In the investigated case the algorithm adapts within 2 s and is then accurately ensuring compatibility. The adaption time is depending on the properties of the coupled components. Figure 2.7 shows the comparison of the displacement of mass 4 with the reference overall system. After the adaption process the reference system is simulated accurately. In all of our numerical studies the algorithm was found to be very robust. As indicated by Fig. 2.8 noisy force and displacement signals have little impact on adaption time and stability issues in this numerical case study which indicates a good feasibility for practical implementation.

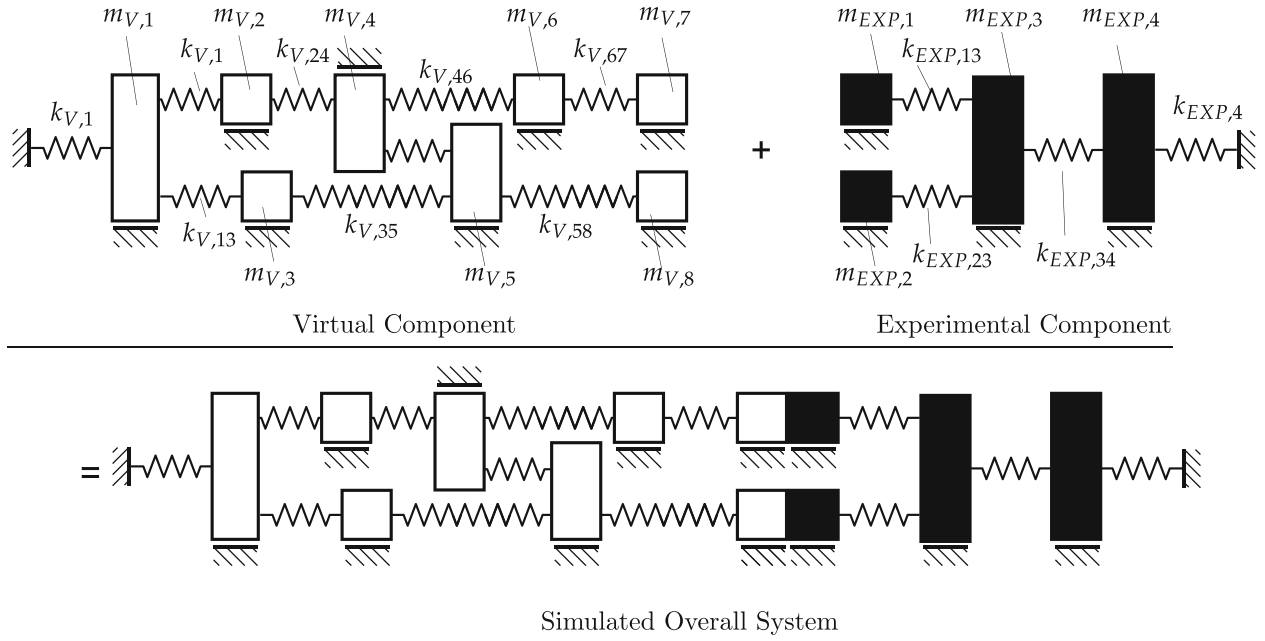


Fig. 2.4 Arrangement of the lumped mass system used for numerical studies

Table 2.1 System parameters used in the numerical case study

Virtual component (V)			
Stiffness (N/m)		Mass (kg)	
$k_{V,1}$	25,000,000	$m_{V,1}$	10
$k_{V,12}$	10,000,000	$m_{V,2}$	3
$k_{V,13}$	10,000,000	$m_{V,3}$	3
$k_{V,24}$	10,000,000	$m_{V,4}$	3
$k_{V,35}$	10,000,000	$m_{V,5}$	3
$k_{V,45}$	10,000,000	$m_{V,6}$	2
$k_{V,58}$	500,000	$m_{V,7}$	2
$k_{V,46}$	20,000,000	$m_{V,8}$	4
$k_{V,67}$	20,000,000		
Test specimen (EXP)			
Stiffness (N/m)		Mass (kg)	
$k_{EXP,13}$	2,500,000	$m_{EXP,1}$	2
$k_{EXP,23}$	2,000,000	$m_{EXP,2}$	4
$k_{EXP,34}$	10,000,000	$m_{EXP,3}$	8
$k_{EXP,4}$	10,000,000	$m_{EXP,4}$	5

2.5 Conclusion

In this paper we propose an adaptive feedforward technique with harmonic regressor for interface synchronization in Real Time Hybrid Testing. The approach makes use of the assumption of harmonic excitation and steady state. It addresses stability and accuracy issues in cases where the simulated overall system is a structural system with low damping. Multiple DoF interfaces are necessary in many applications. As the choice of adaption gain parameters is getting a complex task for tests with multiple DoF interfaces, we propose the use of a recursive least square algorithm for the adaption of the harmonic parameters with only a single parameter for the controller design. Future work will include the experimental validation on a test rig with a multiple DoF interface as well as the comparison with other interface synchronization techniques for Real Time Hybrid Testing.

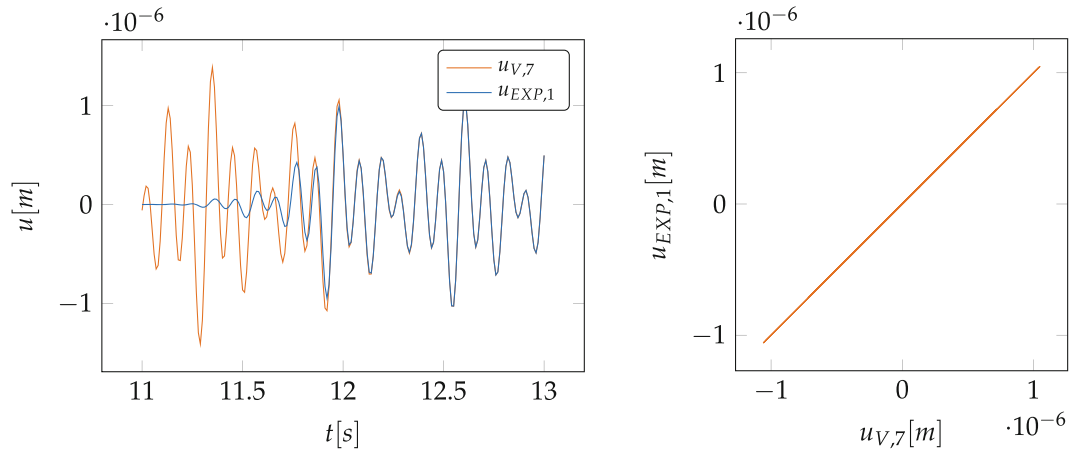


Fig. 2.5 Interface synchronization for the first interface DoF: the *left hand figure* shows the adaption process, the *right hand figure* shows the synchronization in the adapted state

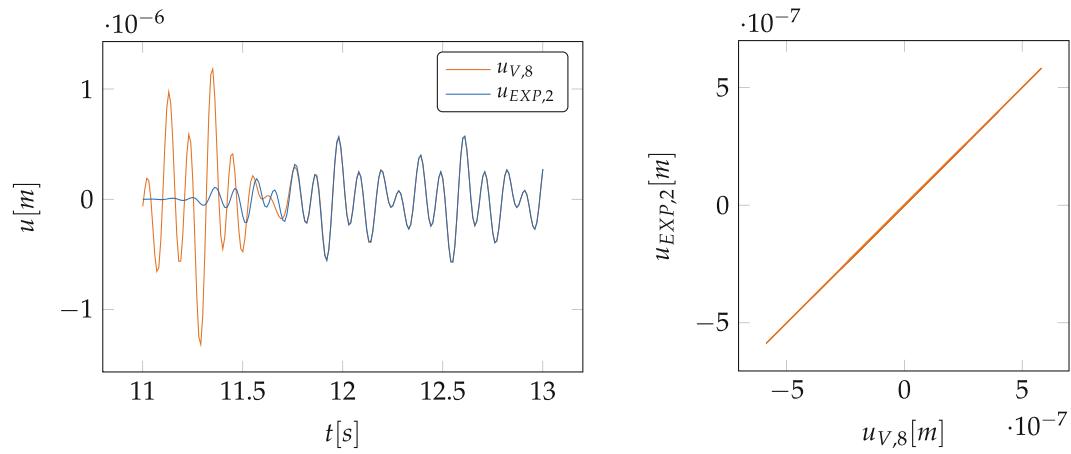


Fig. 2.6 Interface synchronization for the second interface DoF: the *left hand figure* shows the adaption process, the *right hand figure* shows the synchronization in the adapted state

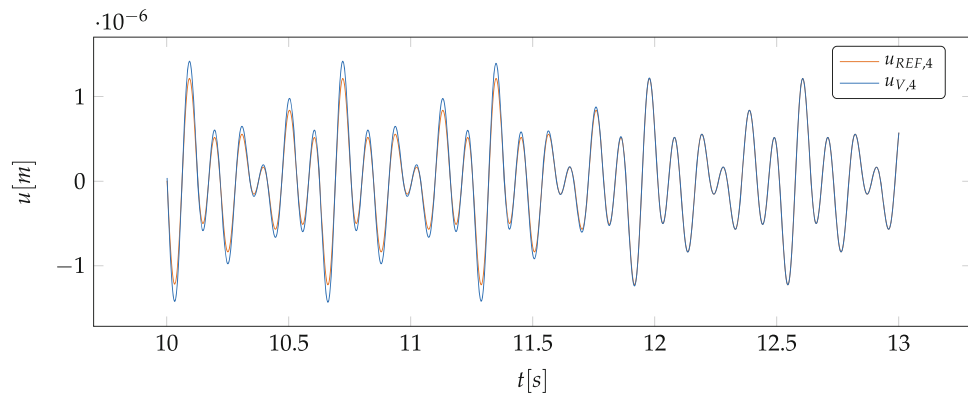


Fig. 2.7 Displacement of mass 4 during the adaption process compared with the reference overall system

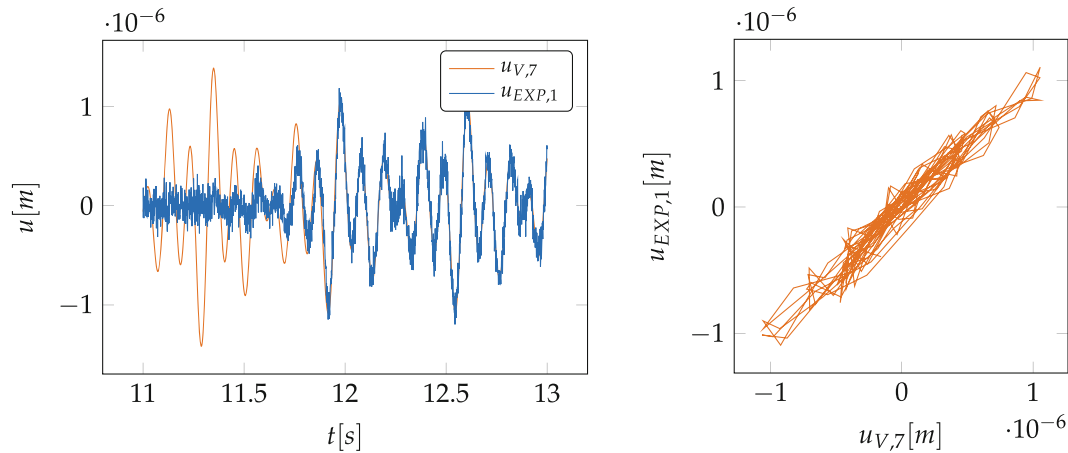


Fig. 2.8 Interface synchronization for the first interface DoF with added noise on force and displacement signals: the *left hand figure* shows the adaption process, the *right hand figure* the synchronization in the adapted state

References

1. Bartl, A., Mayet, J., Rixen, D.J.: Adaptive feedforward compensation for real time hybrid testing with harmonic excitation. In: Proceedings of the 11th International Conference on Engineering Vibration, Sept 2015
2. Bayard, D.S.: A general theory of linear time-invariant adaptive feedforward systems with harmonic regressors. *IEEE Trans. Autom. Control* **45**(11), 1983–1996 (2000)
3. Blakeborough, A., Darby, A., Williams, M.: The development substructure of real-time testing. *Philos. Trans. Math. Phys. Eng. Sci.* **359**(1786), 1869–1891 (2001)
4. Bodson, M., Sacks, A., Khosla, P.: Harmonic generation in adaptive feedforward cancellation schemes. *IEEE Trans. Autom. Control* **39**(9), 1939–1944 (1994)
5. Bonnet, P.A.: The development of multi-axis real-time substructure testing. Ph.D. thesis (2006)
6. Bosse, D., Radner, D., Schelenz, R., Jacobs, G.: Analysis and application of hardware in the loop wind loads for full scale Nacelle ground testing. *DEWI Mag.* **43**, 65–70 (2013)
7. Botelho, R.M., Christenson, R.E.: Mathematical equivalence between dynamic substructuring and feedback control theory. In: Proceedings of the 33rd IMAC (2015)
8. Darby, A.P., Williams, M.S., Blakeborough, A.: Stability and delay compensation for real-time substructure testing. *J. Eng. Mech.* **128**, 1276–1284 (2002)
9. De Klerk, D., Rixen, D.J., Voormeeren, S.N.: General framework for dynamic substructuring: history, review and classification of techniques. *AIAA J.* **46**(5), 1169–1181 (2008)
10. Glover, J.: Adaptive noise canceling applied to sinusoidal interferences. *IEEE Trans. Acoust. Speech Signal Process.* **25**, 484–491 (1977)
11. Haykin, S.: *Adaptive Filter Theory*. Upper Saddle River, Prentice Hall (2010)
12. Horiuchi, T., Inoue, M., Konno, T., Namita, Y.: Real-time hybrid experimental system with actuator delay compensation and its application to a piping system with energy absorber. *Earthq. Eng. Struct. Dyn.* **28**(10), 1121–1141 (1999)
13. Ioannou, P., Sun, J.: *Robust Adaptive Control*. Dover Publications, New York (2013)
14. Jungblut, T., Wolter, S., Matthias, M., Hanselka, H.: Using numerical models to complement experimental setups by means of active control of mobility. *Appl. Mech. Mater.* **70**, 357–362 (2011)
15. Li, G.: A generic dynamically substructured system framework and its dual counterparts, pp. 10101–10106 (2014)
16. Li, G., Na, J., Stoten, D.P., Ren, X.: Adaptive neural network feedforward control for dynamically substructured systems. *IEEE Trans. Control Syst. Technol.* **22**(3), 944–954 (2014)
17. Nakashima, M., Kato, H., Takaoka, E.: Development of real-time pseudo dynamic testing. *Earthq. Eng. Struct. Dyn.* **21**, 79–92 (1992)
18. Plummer, A.: Model-in-the-loop testing. *Proc. Inst. Mech. Eng. I: J. Syst. Control Eng.* **220**, 183–199 (2006)
19. Stoten, D., Hyde, R.: Adaptive control of dynamically substructured systems: the single-input single-output case. *Proc. Inst. Mech. Eng. I: J. Syst. Control Eng.* **220**(2), 63–79 (2006)
20. Stoten, D., Li, G., Tu, J.: Model predictive control of dynamically substructured systems with application to a servohydraulically actuated mechanical plant. *IET Control Theory Appl.* **4**(2), 253–264 (2010)
21. Stoten, D., Tu, J., Li, G.: Synthesis and control of generalized dynamically substructured systems. *Syst. Control Eng.* **223**, 371–392 (2010)
22. Tu, J.: Development of numerical-substructure-based and output-based substructuring controllers. In: *Structural Control and Health Monitoring*, June 2012, pp. 918–936. Wiley, New York (2013)
23. Wagg, D.J., Stoten, D.P.: Substructuring of dynamical systems via the adaptive minimal control synthesis algorithm. *Earthq. Eng. Struct. Dyn.* **30**(6), 865–877 (2001)
24. Wallace, M.I., Wagg, D.J., Neild, S.a.: An adaptive polynomial based forward prediction algorithm for multi-actuator real-time dynamic substructuring. *Proc. R. Soc. A Math. Phys. Eng. Sci.* **461**(2064), 3807–3826 (2005)

Dynamics of Coupled Structures, Volume 4
Proceedings of the 34th IMAC, A Conference and
Exposition on Structural Dynamics 2016

Allen, M.; Mayes, R.L.; Rixen, D. (Eds.)

2016, IX, 528 p. 446 illus., 353 illus. in color., Hardcover

ISBN: 978-3-319-29762-0